



Mechanistic study on the facilitation of enzymatic hydrolysis by α -glucosidase in the presence of betaine-type metabolite analogs



Yuichi Nakagawa^a, Shiro Sehata^a, Satoshi Fujii^a, Hiroaki Yamamoto^b, Akihiko Tsuda^b, Kazuya Koumoto^{a,c,*}

^a Department of Nanobiochemistry, FIRST (Frontiers of Innovative Research in Science and Technology), Konan University, 7-1-20 Minatojima-minamimachi, Chuo-ku, Kobe 650-0047, Japan

^b Department of Chemistry, Graduate School of Science, Kobe University, 1-1 Rokkodai-cho, Nada-ku, Kobe 657-8501, Japan

^c FIBER (Frontier Institute for Biomolecular Engineering Research), Konan University, 7-1-20 Minatojima-minamimachi, Chuo-ku, Kobe 650-0047, Japan

ARTICLE INFO

Article history:

Received 30 January 2014

Received in revised form 7 June 2014

Accepted 7 June 2014

Available online 12 June 2014

ABSTRACT

Recently we reported that betaine-type metabolite analogs structure-dependently facilitate enzymatic hydrolysis reaction for α -glucosidases, β -glucosidases, and alkaliphosphatases. To understand the facilitation mechanism for enzymes, in this study we expanded the analog library and measured the properties of analog solutions. The structural investigation on α -glucosidase-mediated hydrolysis reaction indicated that suitable structures to facilitate the enzyme reaction efficiently should have the ammonium cation in the betaine structure possess triplicate aliphatic chains from C1 to C7 without any polar functional groups. Analyses of the solution properties revealed that such analogs possess a large hydration layer with low water density. Such a specific hydration environment is generated by the characteristic structure of the betaine-type metabolite analogs. The characteristic hydration indirectly regulates enzyme activity and stability. These findings not only increase our understanding enzyme activation by betaine-type metabolite analogs, but also will contribute to the molecular design of enzyme regulators.

© 2014 Elsevier Ltd. All rights reserved.

1. Introduction

Enzymes are one of the most ecological and useful catalysts under ambient conditions and have extensively been investigated for use in biological, diagnostic, and industrial fields. However, the low activity and stability of enzymes is sometimes a problem. Therefore, the enhancement of the enzymatic activity and stability is of great significance. In order to obtain active and stable enzymes, several strategies have been reported, such as screening new enzymes from natural sources,¹ site-specific mutations of enzymes utilizing genetic engineering,^{1,2} the addition of organic molecules into the reaction buffer,^{3–16} and so on. Above all, the addition of organic molecules in the reaction buffer is particularly useful because it is easy and inexpensive. As organic additives, cellular small molecules, such as amino acids, polyols, and various metabolites have been used.^{8–16} Some metabolites are specifically accumulated in cells when they face extremely harsh conditions.¹⁷ Under such conditions, the concentration of metabolites sometimes reaches

several mol/L yet they do not significantly inhibit cellular functions.^{18,19} This ability may be exploited to improve enzymatic activation and stabilization.

To investigate the molecular function of metabolites, we recently synthesized an analog library²⁰ (Fig. 1) derived from the naturally-occurring metabolite glycine betaine (2-*N,N,N*-trimethylammonium acetate), which is a common metabolite found in microorganisms, animals, and plants.¹⁷ We modified the chemical structure in ways analogous to natural changes in cellular metabolite structures; that is, changed the linker length in compound **1** (glycine betaine) between the ammonium cation and carboxylate anion (analog **2**, **3**), changed the bulkiness of the ammonium group (analog **4–8**), or changed the number of intramolecular zwitterions (analog **9**) (Fig. 1). We found that these analogs structure-dependently regulate the thermal stability of DNA duplexes.²⁰

A subsequent study revealed that these analogs increase enzymatic activity just by dissolving them into the reaction buffer.²¹ A kinetic study using α -glucosidase revealed that the activating effect of the analogs worked not only by enhancing the rate constant but also by improving thermostability, salt tolerance, and substrate specificity. Interestingly, enzyme activation was commonly

* Corresponding author. Tel.: +81 78 303 1465; fax: +81 78 303 1495; e-mail address: koumoto@center.konan-u.ac.jp (K. Koumoto).

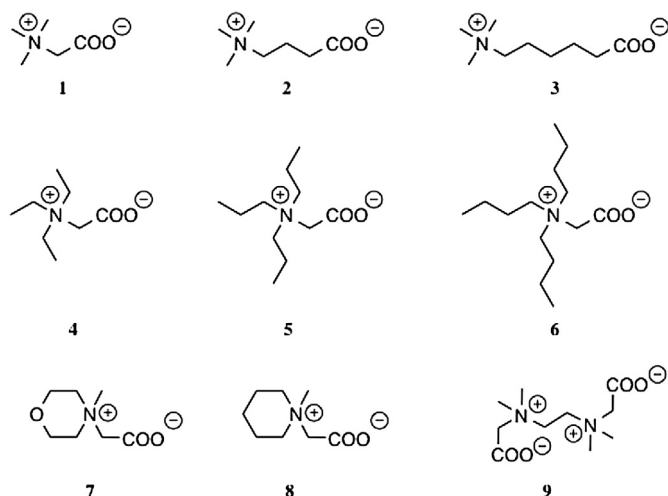


Fig. 1. Chemical structure of metabolite analogs derived from glycine betaine.

observed for different types of hydrolases, such as α -glucosidase, β -glucosidase, and alkaline phosphatase. Furthermore, the facilitation of enzymatic hydrolysis strongly depended on the chemical structure and the concentration of the analogs. In particular, efficient

linker length between the ammonium cation and carboxylate anion. Taking structural differences into consideration, we designed analogs **2** and **3**. Similarly, to assess the bulkiness of the ammonium cation, analogs **4–6** were designed. Also, to assess functional groups introduced into the ammonium cation, analogs **4**, **7**, and **8** were designed, which have similar bulkiness but different functional groups attached to the ammonium group. However, the changes in these compounds do not have major structural consequences.

We therefore newly designed and synthesized analogs **10–21** (Fig. 2). Our previous study revealed that analogs **4–6**, which possess aliphatic chains attached to the ammonium cation, strongly accelerated enzymatic hydrolysis, and the acceleration was intensified as the aliphatic chains become longer. Therefore, long aliphatic chains introduced into the ammonium cation may be important in the facilitation of enzymatic hydrolysis. Eight analogs (**10–17**) were synthesized to test this. Analog **10** possesses triplicate *n*-pentyl, *n*-hexyl, *n*-heptyl, and *n*-octyl chains in the ammonium cation, respectively. They have more bulky ammonium cation moieties than analogs **4–6**. In addition, in order to investigate, which of the introduced aliphatic chains affects enzymatic activity, analogs **14–17** were synthesized. Analog **14** and **15** have duplicate *n*-hexyl chains and either one *n*-butyl or one *n*-octyl chain attached to the ammonium cation, and analogs **16** and **17** have duplicate *n*-butyl chains and either one methyl or one *n*-octyl chain.

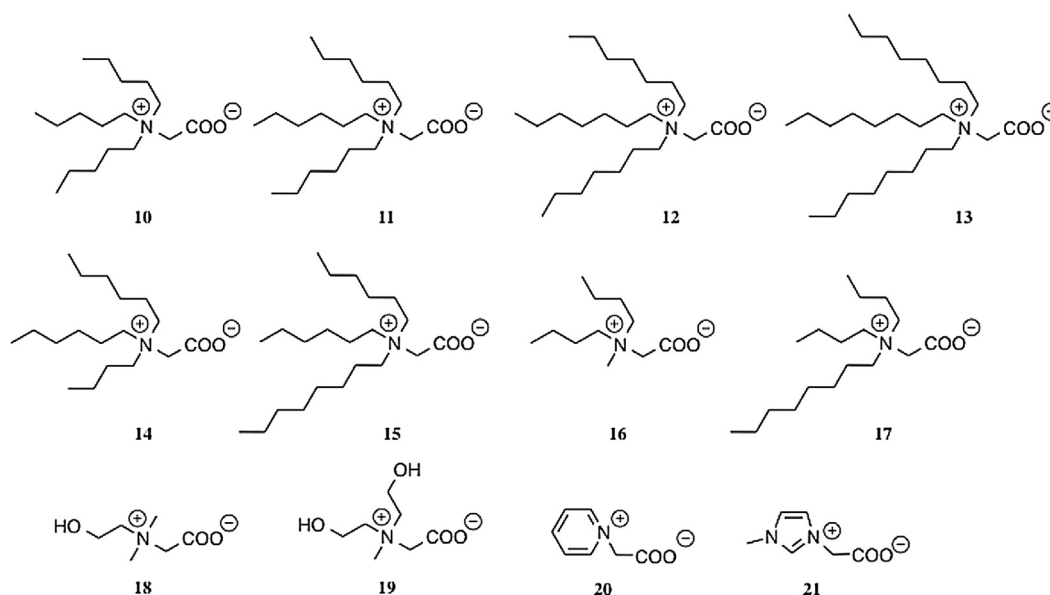


Fig. 2. Chemical structure of newly synthesized metabolite analogs.

facilitation was achieved by analogs possessing relatively long aliphatic chains containing the ammonium cation. However, we did not obtain any information as to why the analogs structure-dependently facilitated enzymatic reactions. In the current study, we expanded the library of analogs to clarify the structural contribution to the facilitation of enzymatic hydrolysis and investigated the mechanism.

2. Results and discussion

2.1. Metabolite analog library expansion

The molecular design of the metabolite analogs derived from glycine betaine (analog **1**) was based on the structural diversity of naturally occurring cellular metabolites. For example, glycine and β -alanine, which are both naturally-occurring metabolites, differ in

Our previous study also suggested that having a polar group as part of the ammonium cation, such as in analog **7**, diminishes the enzymatic activation compared with aliphatic analogs that possess similar bulkiness (analog **4** and **8**).²¹ However, it was difficult to conclude whether structural effects caused by the introduced functional groups were responsible. Therefore, we added analogs that possess other functional groups (**18–21**). Analog **18** and **19**, which have one or two hydroxyl groups at the end of the hydrocarbon, were synthesized to test the influence of polar functional groups in the ammonium cation. Analog **20** and **21** were synthesized to test the influence of aromaticity in the ammonium cation.

2.2. Synthesis and water-solubility of analogs

All of the analogs (**10–19**) were synthesized according to the previously reported method.²⁰ All compounds were confirmed

with ^1H nuclear magnetic resonance (NMR), ^{13}C NMR, Fourier transform-infrared (FTIR), and high resolution electrospray ionization mass (HR-ESI-MS) spectroscopies (the spectra are shown in the electronic Supplementary data (ESD)).

We first tested the water solubility of the analogs. Water solubility was tested by unfavorable turbidity increases in aqueous analog solutions and is summarized in Table 1. When the aliphatic chain was short, from C_1 to C_5 , the water solubility did not change significantly (more than 3000 mM). In contrast, the water solubility for analogs **11** (C_6), **12** (C_7), and **13** (C_8) dropped to 30 mM, 0.3 mM, and nearly 0 mM, respectively, suggesting that when the aliphatic chains become longer than C_6 , hydrophobicity appears. The water solubilities of analogs **14**, **16**, and **17**, whose total carbon numbers in the ammonium cation are smaller than that of analog **11**, were more than 3000 mM, whereas that of analog **15** dropped (1.5 mM) and was close to that of analog **12**, suggesting that the total carbon number of the ammonium cation determines the water solubility of the analogs.

Table 1
Water-solubility of the synthetic analogs

Analog	Water-solubility (mM)	Total carbon number in an ammonium cation
Analog 1	>3000	3
Analog 2	>3000	3
Analog 3	>3000	3
Analog 4	>3000	6
Analog 5	>3000	9
Analog 6	>3000	12
Analog 7	>3000	5
Analog 8	>3000	6
Analog 9	1500	3 ^b
Analog 10	3000	15
Analog 11	30	18
Analog 12	0.3	21
Analog 13 ^a	≈ 0 ^a	24
Analog 14	3000	16
Analog 15	1.5	20
Analog 16	>3000	9
Analog 17	>3000	16
Analog 18	>3000	4
Analog 19	>3000	5
Analog 20	>3000	5
Analog 21	>3000	4

^a Analog **13** did not dissolve in water even at 0.05 mM.

^b Six carbons are divided in two ammonium groups.

2.3. Enzymatic activity in the presence of analogs

Fig. 3a shows the activity (activity=initial velocity in the presence of analog/initial velocity in the absence of analog) of the hydrolysis reaction by α -glucosidase as a function of the analog

concentrations using analogs **1**, **4–6**, **10–12**, **14–17** (Fig. 3b shows activity over a low concentration range from 0 to 1.0 mM). As shown in the figure, the activation behavior is altered by the chemical structures of the metabolite analogs. For analogs **1** and **4**, the activity linearly increases as the analog concentration increases, and the maximal activities are 1.33 and 2.21 at 1000 mM, respectively. On the other hand, when the alkyl chains are longer than triplicate ethyl (C_2) chains (analog **4**), a concentration-dependent activation behavior (bell-type plots) is observed. For analog **5**, the maximal activity (3.36) appeared at 500 mM. As the chain length becomes longer than that of analog **5**, the analog concentrations that induce the maximal activation of enzymatic hydrolysis shift to lower concentrations: the maximal activation concentrations for analogs **6**, **10**, **11**, **12**, **14**, **15**, **16**, and **17** appeared around 100 mM (4.27), 5 mM (3.96), 0.5 mM (2.99), 0.05 mM (2.15), 1 mM (3.43), 0.1 mM (2.71), 100 mM (3.23), and 1 mM (3.37), respectively (maximal activities are noted in parentheses). As being consistent with the previous study,²¹ the activation observed for the synthetic analogs is ascribed to both decrease in K_m and increase in V_{max} (ESD, Table S1).

To understand the relationship between the total carbon number of triplicate aliphatic chains introduced into the ammonium cation and either the maximal activation concentration or maximal activity, we plotted them in Fig. 4a and b, respectively. As shown in Fig. 4a, the maximal activation concentration linearly decreased as the total carbon number increased. On the other hand, the maximal activities describe a bell-shape curvature with analog **6** at the top (Fig. 4b).

We also assessed the influence of the identity of the introduced aliphatic chains using analogs **14**, **15–17**. With respect to the maximal activation concentration, the plots do not show any relationship for analogs **5**, **6**, **10–12** and total carbon number in the ammonium cation. The maximal activation concentration for analogs **16** and **17** is altered by the contribution of another chain; the concentration for analog **16** (duplicate *n*-butyl chains and one methyl chain) is the equal to that for analog **6** (triplicate *n*-butyl chains), suggesting that the duplicate *n*-butyl chains form the dominant structure and that the contribution of the methyl chain is negligible. In contrast, the maximal concentration for analog **17** shifted to 100-fold lower than those of analogs **6** and **16**, suggesting that the longer *n*-octyl chain intensifies the activation effect. Similarly, that for analog **14** possessing duplicate *n*-hexyl chains and one *n*-butyl chain in the ammonium cation was nearly equal to that for analog **11** (triplicate *n*-hexyl chains), whereas that for analog **15** possessing duplicate *n*-hexyl chains and one *n*-octyl chain shifted to 10-fold lower than those of analogs **11** and **14**. These results indicate that introduced short chains scarcely affect the maximal activation concentration, whereas long chains intensify the activation effect.

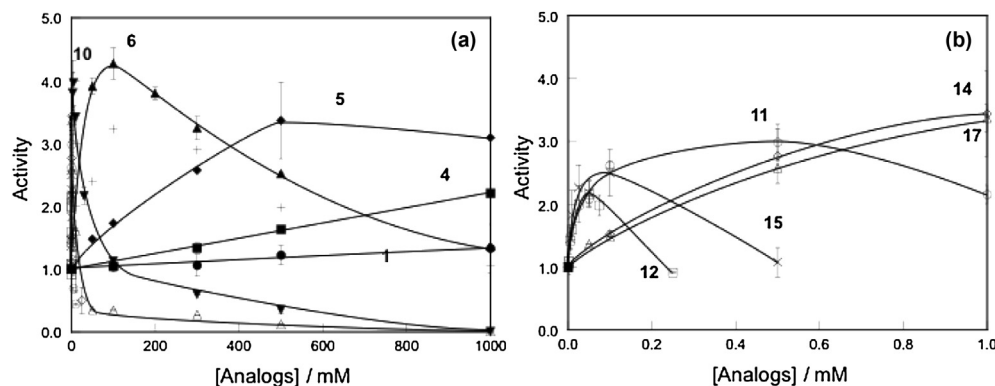


Fig. 3. Plots of activity as a function of the analog concentration for (a) 0–1000 mM and (b) 0–1.0 mM. Analog **1** (filled circle), **4** (filled square), **5** (filled diamond), **6** (filled triangle), **10** (filled inverted triangle), **11** (open circle), **12** (open square), **14** (open diamond), **15** (cross), **16** (plus), and **17** (open triangle).

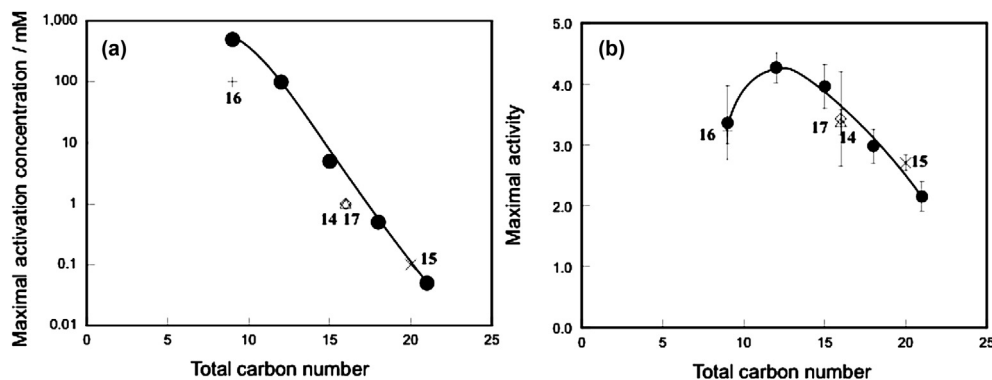


Fig. 4. Relationship between total carbon number of aliphatic chains introduced into ammonium cation and either (a) maximal activation concentration or (b) maximal activity for analogs **5**, **6**, **10–12** (filled circle) and analogs **14** (open diamond), **15** (cross), **16** (plus), and **17** (open triangle).

In contrast, with respect to the maximal activity, analogs **14**, **15–17** obey the relationship between the maximal activities seen for analogs **5**, **6**, **10–12** and the total carbon number in the ammonium cation. This suggests that the activity is mostly determined by the total carbon number of the analogs, where the identity of the introduced aliphatic chain is not so significant.

2.4. Influence of introduced functional groups in the ammonium cation

Using analogs **4**, **7**, **8**, **18–21**, we then examined the influence of the functional groups introduced into the ammonium cation. For these analogs, the activity linearly increased as the concentration increased from 0 to 1000 mM. Therefore, in order to compare the additional effects of the analogs, the activities at [analog]=1000 mM were represented as bar graphs as shown in Fig. 5.

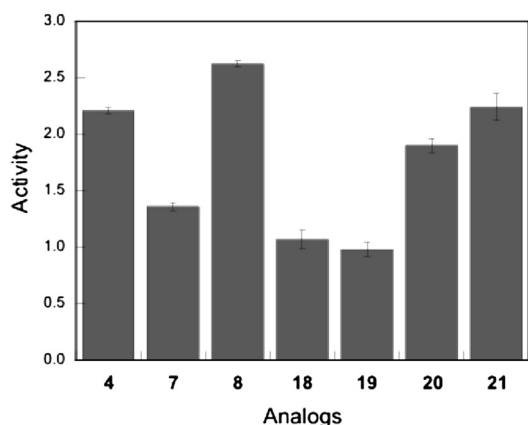


Fig. 5. Comparison of the activity in the presence of analogs **4**, **7**, **8**, **18–21** ([analog]=1000 mM).

Based on molecular dynamics calculations,²² the molecular sizes of analogs **4**, **7**, **8**, **18–21** are similar to each other (the following values are the longest molecular length of each molecule: **4**: 0.69 nm, **7**: 0.63 nm, **8**: 0.65 nm, **18**: 0.77 nm, **19**: 0.77 nm, **20**: 0.75 nm, **21**: 0.82 nm). Therefore, the activity change should be related to the introduced functional group. Similar to our previous study,²¹ the activity in the presence of analog **7** was considerably smaller than those for analogs **4** and **8**. We hypothesized that polar functional groups introduced in the ammonium cation should diminish the activation effect of the analogs. The present results strongly support our hypothesis, given that the activity of analog **18** possessing one hydroxyl group in the ammonium cation was smaller than that of analog **7**, and furthermore, the activity of

analog **19** possessing two hydroxyl groups did not increase activity at all (activity=1). On the other hand, aromatic analogs (**20** and **21**) facilitated enzymatic hydrolysis similar to those of analogs **4** and **8**. In summary, to activate enzymatic hydrolysis, the ammonium cation should be covered with apolar hydrocarbons without any polar functional groups. In this regard, the analogs must be reasonably soluble in aqueous media.

2.5. Comparison of the solution properties of the analogs

To obtain insights as to how these analogs facilitate the enzymatic hydrolysis, we compared their solution properties. Betaine-type metabolite analogs facilitate different hydrolysis reactions catalyzed by α -glucosidases, β -glucosidases, alkaline phosphatases, and DNA polymerases at almost the same concentrations.^{20,21} This feature suggests that the analogs indirectly regulate enzymatic activity rather than engaging specific interactions between enzymes and analogs. We thus compared the solution properties by measuring dynamic light scattering (DLS), osmolarity, water density, and dielectric constants of the analog solutions.

First, to analyze the molecular association behavior of the analogs, DLS measurements were carried out. To obtain reliable scattering intensities, the concentrations of the analogs were adjusted to above 300 mM. DLS measurements therefore were performed for analogs **1**, **4–6**, and **10** whose water solubilities were higher than 300 mM (Table 1). The obtained average grain diameters for the analogs were plotted as functions of the analog concentrations (Fig. 6). For analogs **1**, **4–6**, the average grain diameters did not change over concentration ranges from 300 to 1000 mM, indicating that these analogs were dissolved in aqueous media as monomers.

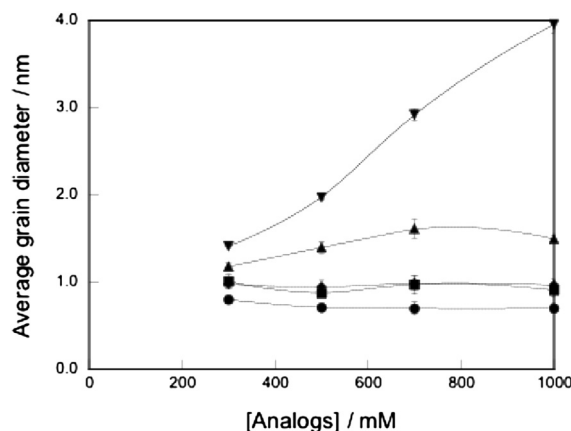


Fig. 6. Plots of average grain diameters estimated from DLS measurements as a function of the analog concentration for analogs **1** (filled circle), **4** (filled square), **5** (filled diamond), **6** (filled triangle), **10** (filled inverted triangle).

On the other hand, the diameter for analog **10** slightly increased from 1.4 nm to 4.0 nm as its concentration increased, indicating that its monomers weakly and dynamically associated together in the aqueous media. This result accounts for the drastic decrease in the water solubility of analogs **11–13** and **15** due to their molecular associations. Additionally, although analog **10** weakly associated in the solution, it dissolved as a monomer at least at the maximal activation concentration (5 mM). This implies that monomer dispersion of the analogs in solution is important to efficiently facilitate the enzymatic reaction.

Based on molecular dynamics calculations,²² the molecular sizes of analogs **1**, **4–6**, and **10** are as follows: **1**: 0.57 nm, **4**: 0.69 nm, **5**: 0.82 nm, **6**: 0.94 nm, and **10**: 1.07 nm. Considering that the molecular sizes measured from DLS (average grain diameters for analogs **1**, **4**, **5**, and **6** are 0.80 ± 0.04 nm, 1.01 ± 0.08 nm, 0.98 ± 0.04 nm, and 1.18 ± 0.04 nm at 300 mM, respectively) were considerably larger than those calculated by molecular dynamics simulations, this suggests the presence of a large hydration layer covering the analogs.

Therefore, we then measured the osmolarity of the analog solutions to estimate their hydration environment. In cells, betaines are well-known osmoprotectants that regulate osmotic pressure by binding water molecules to themselves.^{17–19} The osmolarities of the analog solutions were plotted as a function of the analog concentrations (Fig. 7). As controls, DMSO, glycerol, and glucose were selected because these are representative hydrophilic molecules. As the results show, the osmolarities did not merge with each other, indicating that their hydration environments were different. According to a previous study,^{23,24} as molecules are more hydrated their slopes tend to be larger. In Fig. 7, the slopes of glycerol and glucose are larger than that of DMSO, indicating that the polyols solvated more strongly than DMSO. In contrast, the slopes of the analogs are bent more strongly than those of the controls, indicating that the analogs were hydrated much more so than the hydrophilic control molecules. The order of the slopes is as follows: analogs **5** = **6** > **4** > **1** > **10**. Except for analog **10**, this is in the same order as the enzyme activation. Here, the osmolarity for analog **10** gradually decreased at concentrations above 500 mM. This was due to molecular association, because when the molecules intermolecularly associate, the hydrated water molecules are released from the molecular surface, resulting in a decrease of osmolarity. Compared with the osmolarities for analogs **1**, **4–6**, analogs possessing longer aliphatic chains showed higher osmolarity. However, there was no significant difference between analogs **5** and **6**, although enzymatic activation in the presence of analog **6** is higher than that of analog **5** (Fig. 3).

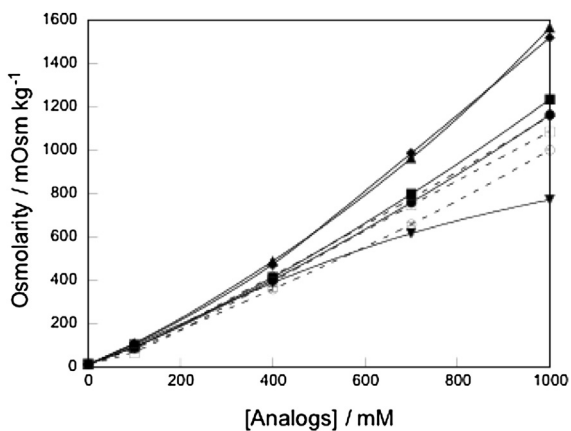


Fig. 7. Plots of osmolarity as a function of the analog concentration for analogs **1** (open circle), **4** (open square), **5** (open diamond), **6** (open triangle), **10** (filled circle), DMSO (open circle), glycerol (open square), and glucose (open diamond).

In order to understand the hydration environment surrounding the analogs, the water density of the analog solutions was measured. As mentioned above, although the osmolarities for analogs **5** and **6** were almost identical, the enzyme activation behavior was different (Fig. 3), suggesting that the hydration environments surrounding the analogs were also different. Ionic compounds are known to hydrate strongly, where water molecules tightly surround the compounds via ion–dipole interactions. In contrast, the charged moiety of the betaine-type analogs is covered with apolar aliphatic chains. Apolar surfaces dislike tightly packed water molecules, which induce unfavorable polarity.^{25,26} Therefore, to solvate betaine-type analogs possessing relatively long aliphatic chains, water should be less tightly packed onto the molecular surface, and furthermore, plenty of water molecules must participate to counteract unfavorable charges via ion–dipole interactions.

Fig. 8 shows plots of the water density for analogs **1**, **4–6** as a function of their concentrations. As the aliphatic chains become longer, the slopes become smaller. As expected, the water densities between analogs **5** and **6** were different, supporting to our hypothesis. The slope of the plots indicates a change in water density accompanying increased analog concentration. In other words, the slope is related to the change of water density of the hydration layer surrounding the analogs. Considering the slope difference between analogs **5** and **6**, the density of hydration water surrounding analog **6** is small.

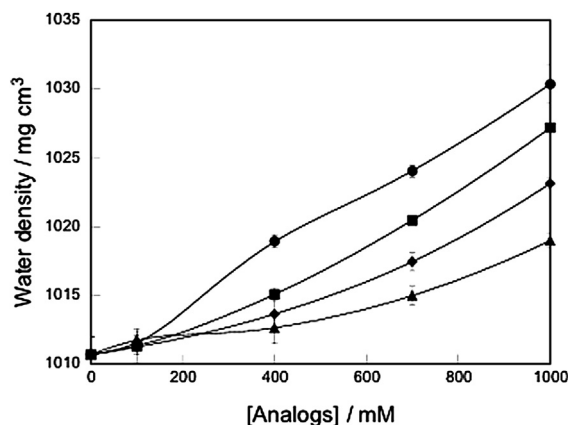


Fig. 8. Plots of water density of the analog-containing aqueous solution as a function of the analog concentration for analogs **1** (filled circle), **4** (filled square), **5** (filled diamond), and **6** (filled triangle).

The present results on the osmolarity and water density of the analog solutions suggest that the analogs, which strongly accelerate α -glucosidase-mediated hydrolysis, possess large hydration layers composed of a low density of hydration water. A large hydration layer possessing low water density, corresponding to a large excluded volume, may eliminate the substrate and enzyme from the area around the analogs, leading to increased collision frequency between substrate and enzyme.

To understand the excluded volume effect, the average grain diameter of α -glucosidase was measured as a function of analog **6** concentration. Fig. 9 shows plots of this. With increased analog concentration, the average grain diameter of analog **6** itself did not change significantly, even in the presence of α -glucosidase, whereas that of α -glucosidase increased as expected. The intermolecular association behavior of α -glucosidase in the presence of analog **6** supports our hypothesis, i.e., analog **6** facilitates molecular interactions owing to the large excluded volume of the hydrated analogs.

Finally, we measured the dielectric constants of the analog solutions. Dielectric constants were measured using 8-anilinonaphthalene sulfonic acid (ANS) as a fluorescence

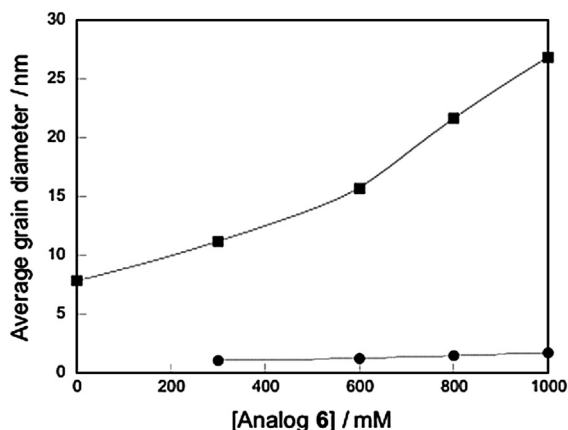


Fig. 9. Plots of the average grain diameter of α -glucosidase (filled square) and analog 6 (filled circle) as a function of analog 6 concentration.

probe.^{27–29} Protein structures are stabilized by Coulomb forces, and therefore, a change in the dielectric constant in the bulk water phase may have an impact on the stability and conformation of the enzyme,^{30,31} resulting in altered enzymatic activity. We plotted the relationship between $1/\epsilon_r$ and the activity of α -glucosidase in Fig. 10. As shown in the figure, there is no relationship between $1/\epsilon_r$ and activity, indicating that the change in the dielectric constant of aqueous media, accompanied by the addition of analogs, does not affect the enzymatic activity. In other words, analogs disperse in aqueous media and are highly solvated with low density hydration water, which is important in enzymatic activation.

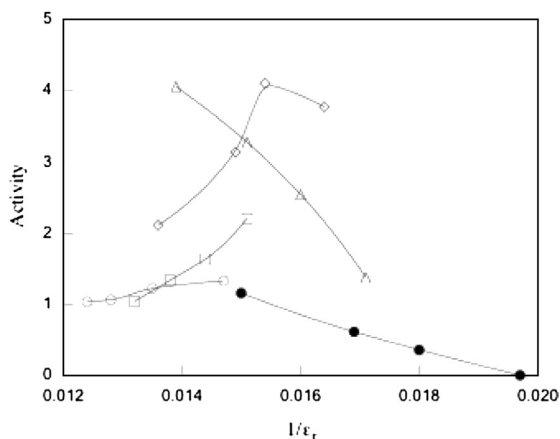


Fig. 10. Plots of $1/\epsilon_r$ as a function of the analog concentration for analogs 1 (open circle), 4 (open square), 5 (open diamond), 6 (open triangle), and 10 (filled circle).

2.6. Influence of outside polar functional groups on the solution properties

To address the question of why introduced polar functional groups to the ammonium cation diminish the enzyme activity, we compared the osmolarities and water densities for aqueous solutions containing analogs 4, 7, 8, 18–21 (Table 2).

Although the changes in osmolarity and water density were too small to compare the values directly, our proposed solvation difference can be observed. For example, a comparison of the values for analogs 7 and 8, whose structural difference consists only of the morpholine moiety being replaced with piperazine, indicates that the polar oxygen atom located outside the molecule increases the water density and decreases the osmolarity, indicating that hydrated water molecules tightly and narrowly packed around the analogs. Also, a comparison of analogs 18 and 19, which possess different numbers of OH groups, revealed that the osmolarity of analog 19 is smaller than that of 18, and the water density of analog 19 is larger than that of 20. These behaviors are analogous. Considering these results, we concluded that solution property changes are related to increased enzymatic activation.

2.7. Theoretical model of enzyme activation by the addition of betaine-type metabolite analogs

According to our previous study,²¹ betaine-type metabolite analogs can facilitate the hydrolysis reaction, which is driven by the enhancement of both the binding affinity between enzyme and substrate (decrease in K_m) and the catalytic activity of the enzyme itself (increase in V_{max}). In addition, the enzyme activation strongly depends on the chemical structures of the analogs added into the reaction buffer. In particular, analogs possessing relatively long aliphatic chains attached to the ammonium cation show profound effects on enzyme activation.

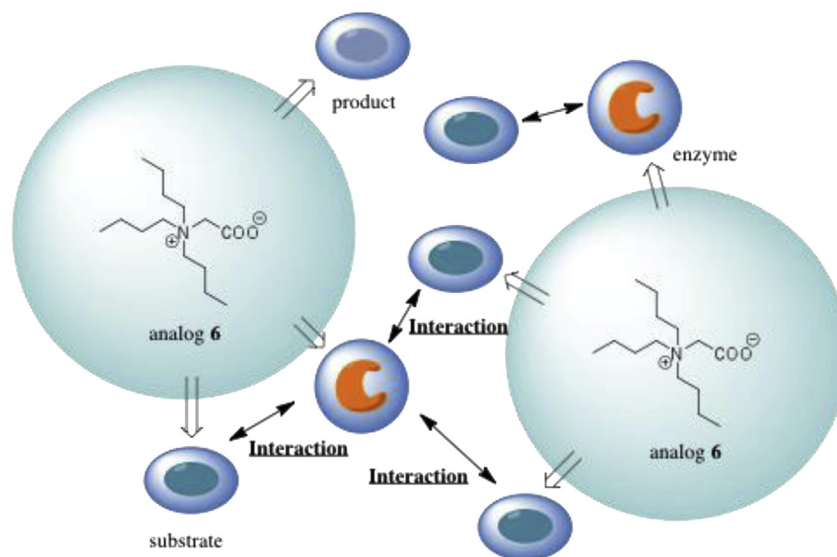
In the present study, we expanded the analog library and found the same structural dependency for enzyme activation as in previous results.²¹ Moreover, we previously showed that betaine-type metabolite analogs facilitate different types of enzymatic reactions catalyzed by α -glucosidases, β -glucosidases, alkaline phosphatases, and DNA polymerases at almost the same concentrations.^{20,21} This suggests that the facilitation effect is not related to specific interactions between enzymes and analogs, but rather to indirect effects. Therefore, we measured the solution properties of analog-containing solutions. Here, we assumed that the hydration of the analogs indirectly regulated the enzymatic reactions by changing the solution properties. First, by measuring the average grain diameters of analogs 1, 4–6, and 10, we revealed that the analogs dissolved in aqueous media as monomers. Furthermore, the osmolarity and water density measurements indicated that the analogs that are good at facilitating enzymatic hydrolysis possess large hydration layers with low water density. Given these results, Scheme 1 represents the effect of analog addition on K_m . The large hydration layer of the analogs provides a large excluded volume in the solution and eliminates the hydrophilic enzyme and substrate from the surface, resulting in the enhancement of collision frequency between substrate and enzyme. This causes an apparent decrease of K_m values in the presence of analogs.

Concurrently, the analogs significantly decrease the water activity in the solution, i.e., they enhance the osmolarity.²³ Previous studies have revealed that the activity and stability of enzymes are highly sensitive to the hydration environment.^{32,33} The large decrease of water activity in the analog solutions alters the hydration balance of the enzyme. This should affect the conformation of α -glucosidase. However, according to our previous study,²¹ CD

Table 2
Comparison of osmolarity, water density, and molecular length of analogs 4, 7, 8, 18–21

Analog	4	7	8	18	19	20	21
Osmolarity/mOsm kg ⁻¹ ^a	1235±4	1162±1	1313±1	1315±7	1232±1	1280±3	1362±2
Water density/mg cm ⁻³ ^a	1027±1	1048±3	1038±1	1047±1	1056±1	1042±2	1047±1
Molecular size/nm	0.69±0.08	0.65±0.01	0.75±0.04	0.80±0.01	0.80±0.01	0.75±0.02	0.82±0.04

^a The values osmolarity and water density are those at [Analog]=1000 mM.



Scheme 1. Schematic illustration of the addition effect of the betaine-type metabolite analogs on K_m .

spectra of α -glucosidase did not change at all even with increasing the analog concentration. It suggests that the activity change is related to the small conformational difference around at active site of α -glucosidase. In fact, when we measured the activation energy of α -glucosidase by Arrhenius plots in the presence of analog **6**, the activation energy was reduced by one-third at [analog **6**]=100 mM (Fig. 11), at which CD spectrum of α -glucosidase is completely merged to that in the absence of analog.²¹ This suggests that a decrease in the water activity alters the conformational flexibility of α -glucosidase.

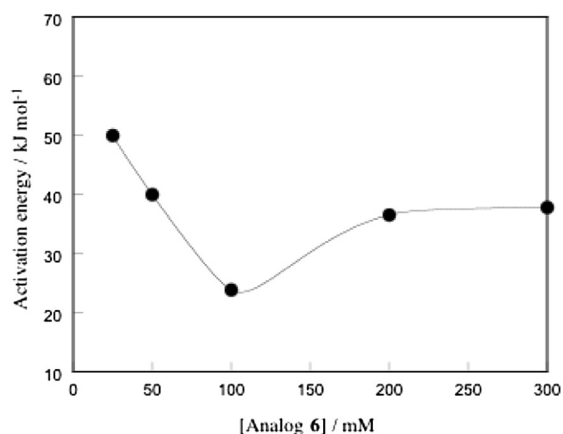


Fig. 11. Plots of activation energy of hydrolysis reaction by α -glucosidase as a function of analog **6** concentration.

3. Conclusions

To understand the mechanism by which betaine-type metabolite analogs facilitate enzymatic hydrolysis, in this study we expanded the analog library and measured the properties of analog-containing solutions. The synthetic analogs structure-dependently facilitated the hydrolysis reaction of α -glucosidase, similar to previous studies.²¹ Our results here indicated that suitable structures to facilitate the enzyme reaction efficiently should have the ammonium cation in the betaine structure possess triplicate aliphatic chains from C₁ to C₇ without any polar functional groups, as the effective concentration for enzyme activation shifts to a lower range as the aliphatic chains become longer. In contrast,

the maximal activity showed a bell-shape curve with analog **6** (triplicate *n*-butyl chains) at the top.

Subsequent analyses of the solution properties revealed that analogs, such as **5** and **6**, which effectively facilitate the enzymatic reaction, were dissolved as monomers and possess a large hydration layer with low water density. Such a specific hydration environment is generated by the characteristic structure of the betaine-type metabolite analogs, whose cationic charge is covered with relatively long apolar hydrocarbons. The characteristic hydration indirectly regulates enzyme activity and stability. These findings not only increase our understanding enzyme activation by betaine-type metabolite analogs, but also will contribute to the molecular design of enzyme regulators.

4. Experimental sections

4.1. Materials

All commercially available reagents and solvents were purchased from Wako Pure Chemicals Ltd. (Osaka, Japan). α -Glucosidases from *Bacillus stearothermophilus* (SIGMA: G3651-250UN) was purchased from SIGMA. They were used without purification unless otherwise noted. All compounds (analogs **10**–**21**) synthesized were synthesized according to a previously reported method²¹ and were characterized by means of ¹H NMR, ¹³C NMR, FTIR, and HR-ESI-MS spectroscopies. ¹H NMR and ¹³C NMR spectra were recorded on a JEOL ECA-500. Chemical shifts were reported with respect to tetramethylsilane (TMS) as the internal standard. FTIR spectra were recorded on a JASCO FT/IR-6300 Fourier transform-infrared spectrometer. HR-ESI-MS spectra were measured on a Fourier Transform Mass Spectrometry (Thermo Fisher Scientific LTQ Orbitrap Discovery). The all spectra were shown in ESD.

4.2. Syntheses

4.2.1. 2-*N,N,N*-Tri-*n*-pentylammonium acetate (10**).** To a solution of tri-*n*-pentylamine (25 mL, 0.09 mol) in ethyl acetate (250 mL) was added 2-bromoacetic acid ethyl ester (8.64 mL, 0.08 mol) and the mixture was stirred at rt for 4 days. The reaction mixture was concentrated to dryness under the reduced pressure and the residue was purified with column chromatography (silicagel CHCl₃/methanol=20:1). Thus obtained light yellow oil was dissolved in H₂O/methanol mixture and was passed through ion-exchange

chromatography (Amberlite IR-402CL). The eluting solution was evaporate to dryness and was dried in vacuo using P₂O₅ to give **10** (18.5 g, 83%) as a light yellow oil: FTIR (ATR) ν/cm^{-1} 2955, 2929, 2872, 1635, 1472, 1340, 1313, 1049, 1033, 840, 717; ¹H NMR (500 MHz, CDCl₃, TMS, rt) δ 0.91 (t, *J*=7.0 Hz, 9H), 1.34 (m, *J*=7.4 Hz, 12H), 1.62 (m, *J*=7.8 Hz, 6H), 3.48 (t, *J*=8.3 Hz, 6H), 3.62 (s, 2H); ¹³C NMR (125 MHz, CDCl₃, TMS, rt) δ 13.87, 21.86, 22.30, 28.58, 58.85, 59.87, 164.40; HR-ESI-MS (positive mode): *m/z* for C₁₇H₃₅NO₂, calculated 286.2746 (MH⁺), found 286.2741 (MH⁺).

4.2.2. 2-(*N,N,N*-Tri-*n*-hexylammonium) acetate (11**).** Compound **11** was obtained in 100% yield as a colorless oil in the same way as for the preparation of **10**: FTIR (ATR) ν/cm^{-1} 2955, 2924, 2858, 1635, 1457, 1363, 1049, 1033, 858, 748, 720; ¹H NMR (500 MHz, CDCl₃, TMS, rt) δ 0.88 (t, *J*=5.8 Hz, 9H), 1.32 (m, 18H), 1.62 (m, 6H), 3.48 (t, *J*=8.0 Hz, 6H), 3.62 (s, 2H); ¹³C NMR (125 MHz, CDCl₃, TMS, rt) δ 13.94, 22.16, 22.48, 26.21, 31.27, 58.90, 59.90, 164.33; HR-ESI-MS (positive mode): *m/z* for C₂₀H₄₁NO₂, calculated 328.3216, found 328.3210 (MH⁺).

4.2.3. 2-(*N,N,N*-Tri-*n*-heptylammonium) acetate (12**).** Compound **12** was obtained in 85% yield as a colorless oil in the same way as for the preparation of **10**: FTIR (ATR) ν/cm^{-1} ; ¹H NMR (500 MHz, CDCl₃, TMS, rt) δ 0.88 (t, *J*=5.8 Hz, 9H), 1.32 (m, 18H), 1.62 (m, 6H), 3.48 (t, *J*=8.0 Hz, 6H), 3.62 (s, 2H); ¹³C NMR (125 MHz, CDCl₃, TMS, rt) δ 14.09, 22.20, 22.53, 26.52, 28.84, 31.58, 58.90, 59.90, 164.31; HR-ESI-MS (positive mode): *m/z* for C₂₃H₄₇NO₂, calculated 370.3685 (MH⁺), found 370.3682 (MH⁺).

4.2.4. 2-(*N,N,N*-Tri-*n*-octylammonium) acetate (13**).** Compound **13** was obtained in 84% yield as a colorless solid in the same way as for the preparation of **10**: Mp 32–33 °C; FTIR (ATR) ν/cm^{-1} 2954, 2919, 2872, 2853, 2360, 1635, 1472, 1363, 1339, 852, 721; ¹H NMR (500 MHz, CDCl₃, TMS, rt) δ 0.87 (t, *J*=6.8 Hz, 9H), 1.28 (m, 30H), 1.61 (m, 6H), 3.47 (t, *J*=7.5 Hz, 6H), 3.62 (s, 2H); ¹³C NMR (125 MHz, CDCl₃, TMS, rt) δ 14.09, 22.20, 22.53, 26.52, 28.84, 31.58, 58.90, 59.90, 164.31; HR-ESI-MS (positive mode): *m/z* for C₂₆H₅₃NO₂, calculated 412.4155 (MH⁺), found 412.4148 (MH⁺).

4.2.5. 2-(*N*-*n*-Butyl-*N,N*-di-*n*-hexylammonium) acetate (14**).** Compound **14** was obtained in 96% yield as a colorless oil in the same way as for the preparation of **10**: FTIR (ATR) ν/cm^{-1} 2956, 2928, 2859, 2363, 2355, 2333, 1635, 1467, 1352, 1313, 1043, 862, 726, 716; ¹H NMR (500 MHz, DMSO-*d*₆, TMS, rt) δ 0.88 (t, *J*=6.0 Hz, 6H), 0.98 (t, *J*=7.0 Hz, 3H), 1.31 (m, 14H), 1.67 (t, 6H), 3.47 (t, 6H), 3.62 (s, 2H); ¹³C NMR (125 MHz, CDCl₃, TMS, rt) δ 13.75, 13.94, 19.93, 22.15, 22.48, 24.17, 26.21, 31.28, 58.69, 58.91, 59.92, 164.32; HR-ESI-MS (positive mode): *m/z* for C₁₈H₃₇NO₂, calculated 300.2903 (MH⁺), found 300.2897 (MH⁺).

4.2.6. 2-(*N,N*-Di-*n*-hexyl-*N*-*n*-octylammonium) acetate (15**).** Compound **15** was obtained in 16% yield as a colorless oil in the same way as for the preparation of **10**: FTIR (ATR) ν/cm^{-1} 2954, 2924, 2857, 1635, 1472, 1340, 1033, 856, 720; ¹H NMR (500 MHz, DMSO-*d*₆, TMS, rt) δ 0.88 (t, 6H), 1.32 (m, 22H), 1.62 (m, 6H), 3.48 (t, *J*=6.8 Hz, 6H), 3.62 (s, 2H); ¹³C NMR (125 MHz, CDCl₃, TMS, rt) δ 13.94, 14.14, 22.14, 22.48, 22.64, 26.21, 26.55, 29.07, 29.12, 31.28, 31.68, 58.90, 59.90, 164.34; HR-ESI-MS (positive mode): *m/z* for C₂₂H₄₅NO₂, calculated 356.3529 (MH⁺), found 356.3522 (MH⁺).

4.2.7. 2-(*N,N*-Di-*n*-butyl-*N*-methylammonium) acetate (16**).** Compound **16** was obtained in 84% yield as a colorless oil in the same way as for the preparation of **10**: FTIR (ATR) ν/cm^{-1} 2961, 2875, 2361, 2342, 1628, 1459, 1378, 1318, 1034, 880, 717; ¹H NMR (500 MHz, DMSO-*d*₆, TMS, rt) δ 0.98 (t, *J*=7.5 Hz, 6H), 1.39 (m, *J*=7.4 Hz, 4H), 1.66 (m, *J*=8.0 Hz, 4H), 3.20 (s, 3H), 3.48 (t, *J*=6.1 Hz, 2H), 3.56 (t, *J*=6.0 Hz, 2H), 3.71 (s, 2H); ¹³C NMR (125 MHz, CDCl₃,

TMS, rt) δ 13.75, 19.88, 24.54, 48.81, 61.90, 62.87, 164.54; HR-ESI-MS (positive mode): *m/z* for C₁₁H₂₃NO₂, calculated 202.1807 (MH⁺), found 202.1801 (MH⁺).

4.2.8. 2-(*N,N*-Di-*n*-butyl-*N*-*n*-octylammonium) acetate (17**).** Compound **17** was obtained in 88% yield as a colorless oil in the same way as for the preparation of **10**: FTIR (ATR) ν/cm^{-1} 2957, 2925, 2858, 2359, 2342, 1635, 1467, 1352, 1311, 1045, 867, 717; ¹H NMR (500 MHz, DMSO-*d*₆, TMS, rt) δ 0.87 (t, *J*=6.8 Hz, 3H), 0.98 (t, *J*=7.5 Hz, 6H), 1.33 (m, 14H), 1.61 (m, *J*=8.0 Hz, 6H), 3.48 (t, *J*=8.5 Hz, 6H), 3.63 (s, 2H); ¹³C NMR (125 MHz, CDCl₃, TMS, rt) δ 13.75, 14.75, 19.93, 22.18, 22.64, 24.17, 26.55, 29.08, 29.13, 31.67, 58.70, 58.91, 59.93, 164.34; HR-ESI-MS (positive mode): *m/z* for C₁₈H₃₇NO₂, calculated 300.2903 (MH⁺), found 300.2896 (MH⁺).

4.2.9. 2-(*N,N*-Dimethyl-*N*-2-hydroxyethylammonium) acetate (18**).** Compound **18** was obtained in 88% yield as a white powder in the same way as for the preparation of **4**:²⁰ Mp 165–167 °C; FTIR (ATR) ν/cm^{-1} 3149, 2362, 2342, 1617, 1390, 1337, 1322, 1063, 990, 922, 894, 786, 768, 715; ¹H NMR (500 MHz, DMSO-*d*₆, TMS, rt) δ 3.11 (s, 6H), 3.54 (s, 2H), 3.57 (t, *J*=5.3 Hz, 2H), 3.73 (br, 2H), 5.21 (br, 1H); ¹³C NMR (125 MHz, methanol-*d*₄, TMS, rt) δ 51.61, 55.88, 64.56, 65.02, 167.66; HR-ESI-MS (positive mode): *m/z* for C₆H₁₃NO₃, calculated 148.0974 (MH⁺), found 148.0965 (MH⁺).

4.2.10. 2-[*N*-Methyl-*N,N*-bis(2-hydroxyethyl)ammonium] acetate (19**).** Compound **19** was obtained in 88% yield as a white powder in the same way as for the preparation of **4**:²⁰ Mp 91–92 °C; FTIR (ATR) ν/cm^{-1} 3399, 3032, 2900, 2839, 2779, 2355, 1600, 1485, 1402, 1340, 1289, 1095, 1008, 910, 872, 819, 726; ¹H NMR (500 MHz, DMSO-*d*₆, TMS, rt) δ 3.15 (s, 3H), 3.60 (s, 2H), 3.66 (m, 4H), 3.74 (br, 4H), 5.25 (t, 2H); ¹³C NMR (125 MHz, methanol-*d*₄, TMS, rt) δ 50.04, 55.73, 62.72, 64.34, 167.92; HR-ESI-MS (positive mode): *m/z* for C₇H₁₅NO₄, calculated 177.1079 (MH⁺), found 178.1074 (MH⁺).

4.2.11. 2-(*N*-Pyridinium) acetate (20**).** Compound **20** was obtained in 60% yield as a white powder in the same way as for the preparation of **4**:²⁰ Mp > 300 °C; FTIR (ATR) ν/cm^{-1} 2967, 2362, 2337, 2165, 2155, 1628, 1485, 1341, 1181, 1051, 1033, 893, 787, 716, 604; ¹H NMR (500 MHz, DMSO-*d*₆, TMS, rt) δ 4.85 (t, 1H), 8.02 (d, *J*=6.5 Hz, 2H), 8.46 (m, *J*=8.0 Hz, 1H), 8.81 (m, *J*=6.0 Hz, 2H); ¹³C NMR (125 MHz, methanol-*d*₄, TMS, rt) δ 63.51, 127.34, 145.00, 145.65, 168.55; HR-ESI-MS (positive mode): *m/z* for C₇H₇NO₂, calculated 138.0555 (MH⁺), found 138.0547 (MH⁺).

4.2.12. 2-(*N'*-Methyl-*N*-imidazolium) acetate (21**).** Compound **21** was obtained in 73% yield as a white powder in the same way as for the preparation of **4**:²⁰ Mp 276–277 °C; FTIR (ATR) ν/cm^{-1} 3033, 2356, 1619, 1562, 1456, 1359, 1294, 1173, 1038, 928, 892, 817, 782, 694, 631; ¹H NMR (500 MHz, DMSO-*d*₆, TMS, rt) δ 3.80 (s, 3H), 4.34 (s, 2H), 7.53 (s, 2H), 8.94 (s, 1H); ¹³C NMR (125 MHz, methanol-*d*₄, TMS, rt) δ 34.97, 51.96, 122.65, 123.55, 137.51; HR-ESI-MS (positive mode): *m/z* for C₆H₈N₂O₂, calculated 141.0664 (MH⁺), found 141.0661 (MH⁺).

4.3. Enzymatic reactions²¹

Enzymatic reactions were performed as follows: a 1 μL aliquot of α -glucosidase stock solution (2.5×10^{-5} mg/mL) was placed onto the wall of each well of a 96-well plate containing 199 μL substrate (0–2.0 mM), metabolite analogs (0–1000 mM) and 100 mM phosphate buffer solution (pH 7.0), and incubated at 37 °C for 3 min. The hydrolysis reaction was started by shaking the plate, thus mixing together the enzyme and buffer. The initial slopes of the absorbance at 405 nm against incubation time were converted into initial velocities using the molar extinction coefficient of *p*-

nitrophenol at 405 nm ($10,900 \text{ cm}^{-1} \text{ M}^{-1}$). The initial velocities were estimated as the average of five measurements.

4.4. DLS measurements

DLS measurements were performed using a Zetasizer Nano (Malvern Instruments Ltd.). The samples were prepared by mixing 100 mM phosphate buffer (pH 7.0) containing 0–1000 mM analog **6** and 5.0 mg/mL α -glucosidase and were measured using a QS 3.00 mm cell.

4.5. Osmolarity measurements

Osmolarities were measured by a Wescor Vapro 5520 vapor pressure osmometer. Fifth measurements of osmolarity were done for each sample at the analog concentration range from 0 to 1000 mM.

4.6. Molecular calculations for synthetic analogs

For molecular dynamics calculations of synthetic analogs **1–21**, the calculations were performed using the Gaussian 03,²² implementing B3LYP functional with double- ζ basis sets 6-31G.

4.7. Estimation of activation energy of α -glucosidase-mediated hydrolysis reaction in the absence and presence of synthetic analogs

To estimate the activation energy of α -glucosidase-mediated hydrolysis reaction, Arrhenius plots were used at the temperature range from 30 to 60 °C. To obtain k_{cat} values, enzymatic reactions at each temperature were performed with changing the analog **6** concentration (0–300 mM). Kinetic parameters were estimated by Hanes–Woolf plots according to the previous study.^{21,34} The typical Arrhenius plot was shown in ESD, Fig. S3.

Acknowledgements

This work was supported in part by Grants-in-Aid for scientific research from the Noguchi Institute, Japan (NJ201005) and the Core Research Project (2009–2014) from the Ministry of Education, Culture, Sports, Science and Technology, Japan.

Supplementary data

Supplementary data related to this article can be found at <http://dx.doi.org/10.1016/j.tet.2014.06.028>.

References and notes

- Arnold, F. H.; Georjoiu, G. In *Directed Enzyme Evolution Screening and Selection Methods Methods Mol. Biol.*; Humana: New Jersey, USA, 2010; Vol. 230, p 3.
- Lutz, S.; Bornscheuer, U. T. In *Protein Engineering Handbook*; Wiley-VCH: Weinheim, Germany, 2012; Vol. 3.
- Goldfeder, M.; Fishman, A. *Appl. Microbiol. Biotechnol.* **2014**, *98*, 545.
- Vathipadiekai, V.; Verma, A.; Rao, M. *Biol. Chem.* **2007**, *388*, 61.
- Moniruzzaman, M.; Nakashima, K.; Kamiya, N.; Goto, M. *Biochem. Eng. J.* **2010**, *48*, 295.
- Kaftzik, N.; Wasserscheid, P.; Kragl, U. *Org. Process Res. Dev.* **2002**, *6*, 553.
- Chiappe, C.; Neri, L.; Pieraccini, D. *Tetrahedron Lett.* **2006**, *47*, 5089.
- Schnoor, M.; Voß, P.; Cullen, P.; Boking, T.; Galla, H.-J.; Galinski, E. A.; Lorkowski, S. *Biochem. Biophys. Res. Commun.* **2004**, *322*, 867.
- Chilson, O. P.; Chilson, A. E. *Eur. J. Biochem.* **2003**, *270*, 4823.
- Chakrabarti, R.; Schutt, C. E. *BioTechniques* **2002**, *32*, 866.
- Henke, W.; Herdel, K.; Jung, K.; Schnorr, D.; Loening, S. A. *Nucleic Acids Res.* **1997**, *25*, 3957.
- Wang, A.; Bolen, D. W. *Biophys. J.* **1996**, *71*, 2117.
- Pomp, D.; Medrano, J. F. *BioTechniques* **1991**, *10*, 58.
- Bowlus, R. D.; Somero, G. N. *J. Exp. Zool.* **1979**, *208*, 137.
- Winship, P. R. *Nucleic Acids Res.* **1989**, *17*, 1266.
- Meecker, A. K.; Li, Y.-K.; Shortle, D.; Stites, W. E. *BioTechniques* **1993**, *15*, 372.
- Yancey, P. H. *J. Exp. Biol.* **2005**, *208*, 2819.
- Yancey, P. H. *Amer. Zool.* **2001**, *41*, 699.
- Yancey, P. H.; Clarl, M. E.; Hand, S. C.; Bowlus, R. D.; Somero, G. N. *Science* **1982**, *217*, 1214.
- Koumoto, K.; Ochiai, H.; Sugimoto, N. *Tetrahedron* **2008**, *64*, 168.
- Deguchi, E.; Koumoto, K. *Bioorg. Med. Chem.* **2011**, *19*, 3128.
- Frisch, M. J.; Trucks, G. W.; Schlegel, H. B.; Scuseria, G. E.; Robb, M. A.; Cheeseman, J. R.; Montgomery, J. A., Jr.; Kudin, K. N.; Burant, J. C.; Millam, J. M.; Iyengar, S. S.; Tomasi, J.; Barone, V.; Mennucci, B.; Cossi, M.; Scalmani, G.; Rega, N.; Petersson, G. A.; Nakatsuji, H.; Hada, M.; Ehara, M.; Toyota, K.; Fukuda, R.; Hasegawa, J.; Ishida, M.; Nakajima, T.; Honda, Y.; Kitao, O.; Nakai, H.; Klene, M.; Li, X.; Knox, J. E.; Hratchian, H. P.; Cross, J. B.; Bakken, V.; Adamo, C.; Jaramillo, J.; Gomperts, R.; Stratmann, R. E.; Yazyev, O.; Austin, A. J.; Cammi, R.; Pomelli, C.; Ochterski, J. W.; Ayala, P. Y.; Morokuma, K.; Voth, G. A.; Salvador, P.; Dannenberg, J. J.; Zakrzewski, V. G.; Dapprich, S.; Daniels, A. D.; Strain, M. C.; Farkas, O.; Malick, D. K.; Rabuck, A. D.; Raghavachari, K.; Foresman, J. B.; Ortiz, J. V.; Cui, Q.; Baboul, A. G.; Clifford, S.; Cioslowski, J.; Stefanov, B. B.; Liu, G.; Liashenko, A.; Piskorz, P.; Komaromi, I.; Martin, R. L.; Fox, D. J.; Keith, T.; Al-Laham, M. A.; Peng, C. Y.; Nanayakkara, A.; Challacombe, M.; Gill, P. M. W.; Johnson, B.; Chen, W.; Wong, M. W.; Gonzalez, C.; Pople, J. A. *Gaussian 03, Revision B.03*; Gaussian: Wallingford CT, 2004.
- Goobes, R.; Kahana, N.; Cohen, O.; Minsky, A. *Biochemistry* **2003**, *42*, 2431.
- Courtenay, E. S.; Capp, M. W.; Anderson, M. W.; Record, M. T., Jr. *Biochemistry* **2000**, *39*, 4455.
- Schobert, B. J. *Theor. Biol.* **1977**, *68*, 17.
- Oleinikova, A.; Brovchenko, I. J. *Phys. Chem. B* **2012**, *116*, 14650.
- Sigel, H.; Martin, R. B.; Tribolet, R. *Eur. J. Biochem.* **1985**, *152*, 187.
- Lazaridis, T.; Karplus, M. *Protein: Struct. Funct. Gen.* **1999**, *35*, 133.
- Wagner, B. D.; MacDonald, P. J. J. *Photochem. Photobiol., A* **1998**, *144*, 151.
- Nandi, N. *Chem. Rev.* **2000**, *100*, 2013.
- Bone, S.; Pethig, R. J. *Mol. Biol.* **1985**, *181*, 323.
- Sellek, G. A.; Chaudhuri, J. B. *Enzyme Microb. Technol.* **1999**, *25*, 471.
- Triantafyllou, A. Ö.; Wehtje, E.; Adlercreutz, P.; Mattiasson, B. *Biotechnol. Bioeng.* **1997**, *54*, 67.
- Burg, M. B.; Peters, E. M.; Bohren, K. M.; Gabbay, K. H. *Proc. Natl. Acad. Sci. U.S.A.* **1999**, *96*, 6517.